

Integrated structure design and synthesis of a pitaya-like SnO₂/N-doped carbon composite for high-rate lithium storage capability

Xiao Liu,^{a,b} Shuai Zhang,^a Peng Zhang,^{*c} Zongmin Zheng,^d Feng Bai^a and Qi Li^{*a}

^aKey Lab for Special Functional Materials of Ministry of Education, National & Local Joint Engineering Research Center for High-efficiency Display and Lighting Technology, Collaborative Innovation Center of Nano Functional Materials and Applications, School of Materials Science and Engineering, Henan University, Kaifeng 475004, P. R. China. *E-mail*: nanokingdom@163.com

^bCollege of Chemistry and Chemical Engineering, Henan Key Laboratory of Function-Oriented Porous Materials, Luoyang Normal University, Luoyang, 471934, P. R. China.

^cDepartment of Chemistry, College of Sciences, Northeastern University, Shenyang, 110819, Liaoning, P. R. China.

^dNational Engineering Research Center for Intelligent Electrical Vehicle Power System, College of Mechanical and Electrical Engineering, Qingdao University, Qingdao, Shandong, 266071, P. R. China.

Physical characterization. The morphology of SnO₂-based nanospheres were observed by Nova Nano SEM 450 microscope. Transmission electron microscope (TEM) images were performed on a JEOL 2010 with 200 kV acceleration voltage. Fourier transform infrared spectroscopy (FTIR) were collected on a VERTEX 70 system (bruker, Gemany). The X-ray diffraction (XRD) patterns were collected with a powder XRD system using Cu Ka radiation (D8-Advance, Bruker, Gemany). Nitrogen adsorption measurements were carried out on Quadrasorb SI-4. XPS studies were measured with an ESCALLAB 250Xi system. Thermogravimetric (TG) analyses were performed on METTLER TOLEDO (DSC851e) under air atmosphere with a heating rate of 10 °C min⁻¹.

Electrochemical measurements. A methyl-2-pyrrolidone (NMP) slurry, consisting of 80 wt% active materials (pitaya-like SnO₂/C@NC, SnO₂/C, yolk-shell SnO₂ or SnO₂/GSSs), 10 wt% of acetylene black, and 10 wt% of polyvinylidene fluoride (PVDF), was coated on a copper foil. Then the slurry was dried at 110°C for 10 h under vacuum, and the loading mass of active materials were controlled about 1.0 mg cm⁻². The cells were assembled in an Ar-filled glove box, Li foil was used as the counter electrode, and 1 M LiPF₆ in ethylene carbonate/diethyl carbonate (EC/DEC 1:1 by volume) was used as electrolyte. Discharge-charge measurements were operated in a voltage range of 0.005-3.0 V. The capacities of samples were calculated based on the mass of SnO₂ active material. Cyclic Voltammograms (CVs) were performed on an Arbin battery test system. The electrochemical impedance spectroscopy (EIS) measurements were

recorded between 0.01 to 10^5 Hz with an excitation voltage of 5 mV. All batteries were test at room temperature.

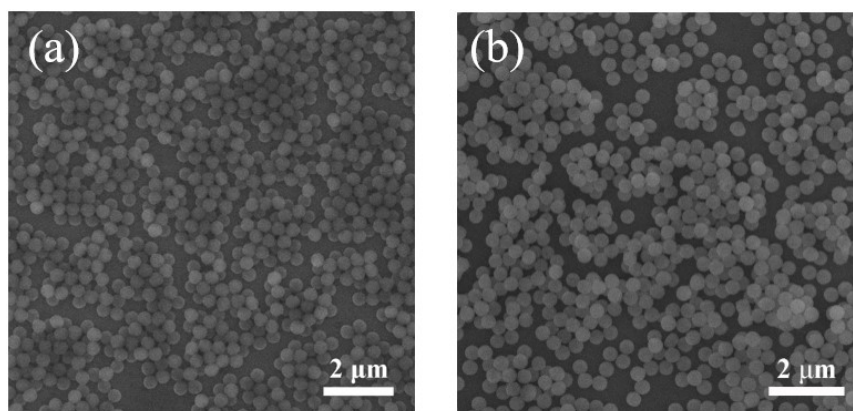


Fig. S1 (a) SEM images of pMS and (b) Sn-pMS.

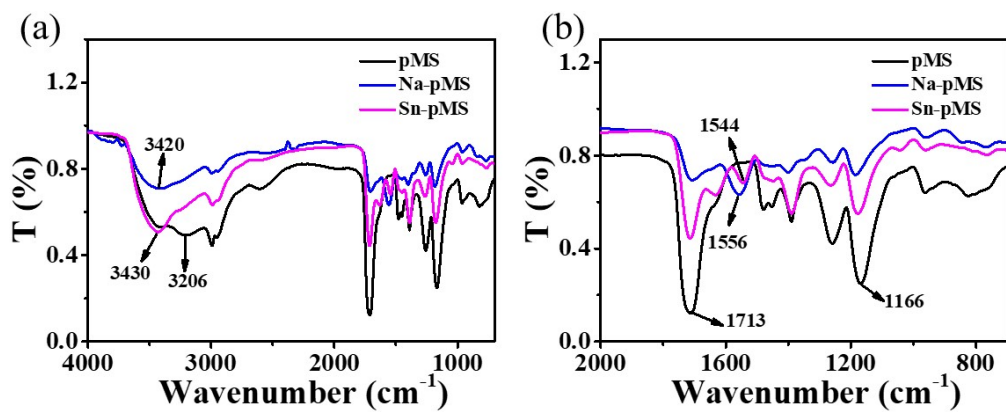


Fig. S2 (a) FTIR spectra of pMS (black), Na-pMS (blue) and after exchange with Sn²⁺ ions (magenta). (b) partial amplification of (a) between 2000 cm⁻¹ and 700 cm⁻¹.

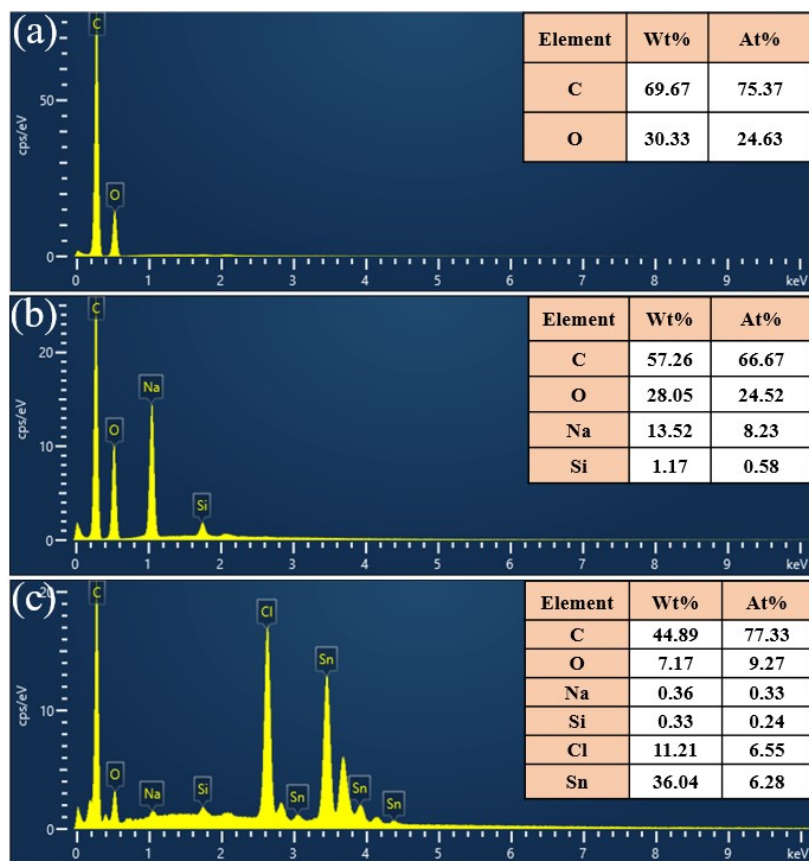


Figure S3 EDS analysis date of (a) pMS, (b) Na-pMS and (c) Sn-pMS.

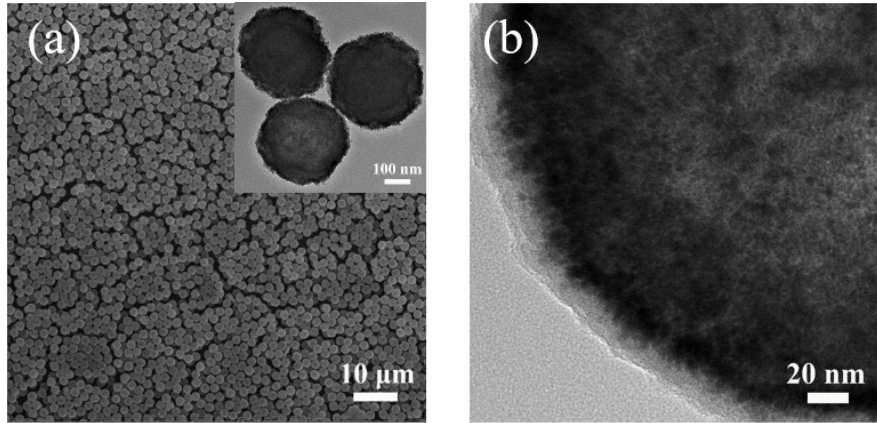


Figure S4 (a) SEM images of monodisperse pre-oxidized nanospheres, (b) TEM image of SnO₂/C@PDA. Insert in (a) is the TEM image of monodisperse pre-oxidized nanospheres.

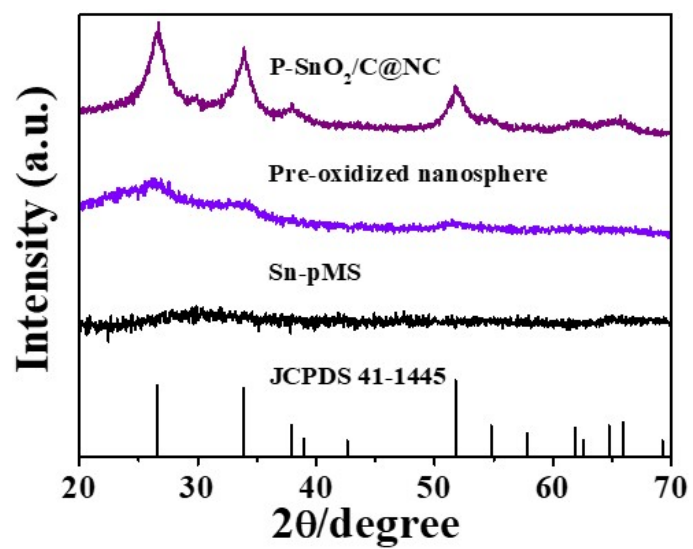


Fig. S5 XRD pattern of Sn-pMS (black line), pre-oxidized nanosphere (violet line) and the obtained P-SnO₂/C@NC (purple line).

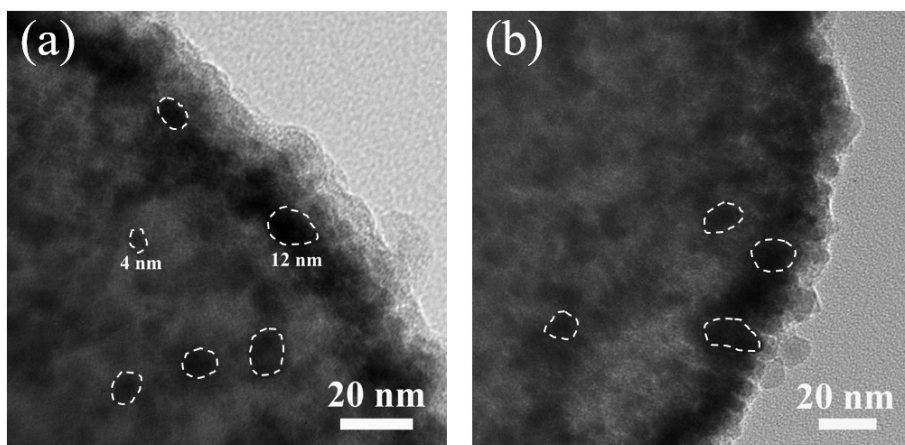


Fig. S6 (a, b) Large scale HRTEM images of P-SnO₂/C@NC.

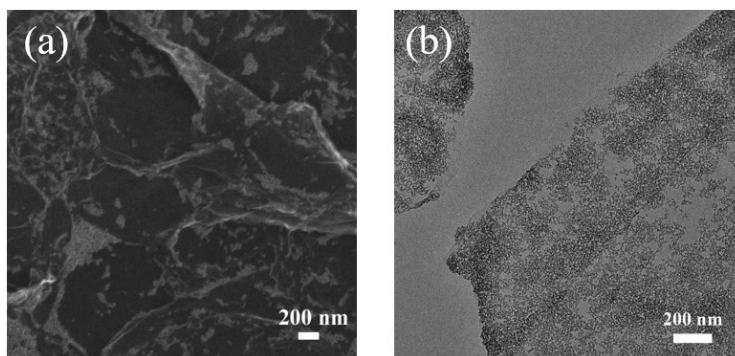


Fig. S7 (a) SEM and (b) TEM images of SnO₂/GSs.

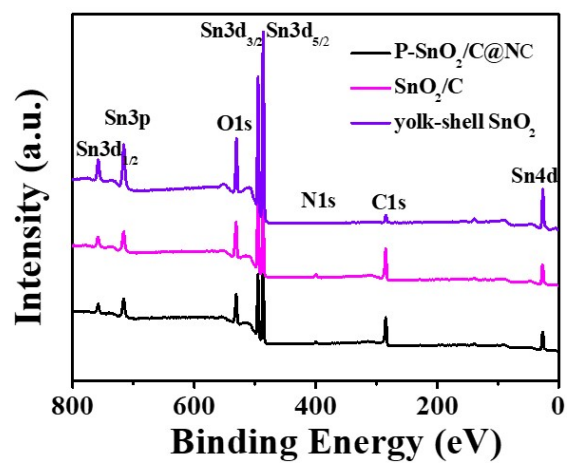


Fig. S8 XPS of spectra of P-SnO₂/C@NC, SnO₂/C and yolk-shell SnO₂.

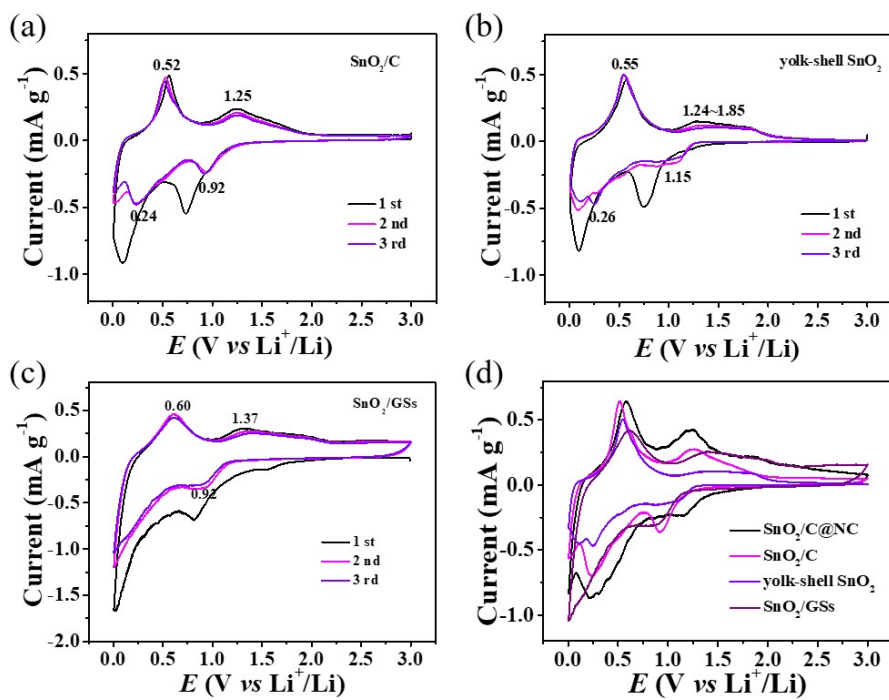


Fig. S9 CV Curves of the initial three cycles of (a) SnO₂/C, (b) yolk-shell SnO₂ and (c) SnO₂/GSSs electrodes between 5 mV and 3.0 V at a scan rate of 0.1 mV s⁻¹. (d) The third cycle of P-SnO₂/C@NC, SnO₂/C, yolk-shell SnO₂ and SnO₂/GSSs electrodes.

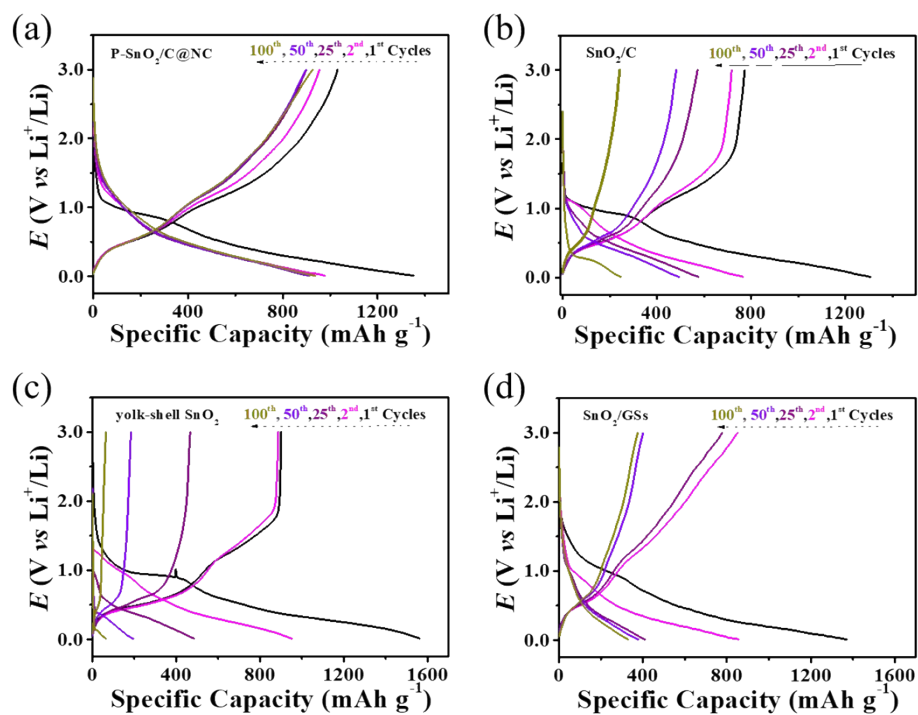


Fig. S10 Charge-discharge voltage profiles of (a) P-SnO₂/C@NC, (b) SnO₂/C, (c) yolk-shell SnO₂ and (d) SnO₂/GSs electrodes in the voltage range of 0.005-3 V vs. Li⁺/Li at a current density of 0.1 A g⁻¹.

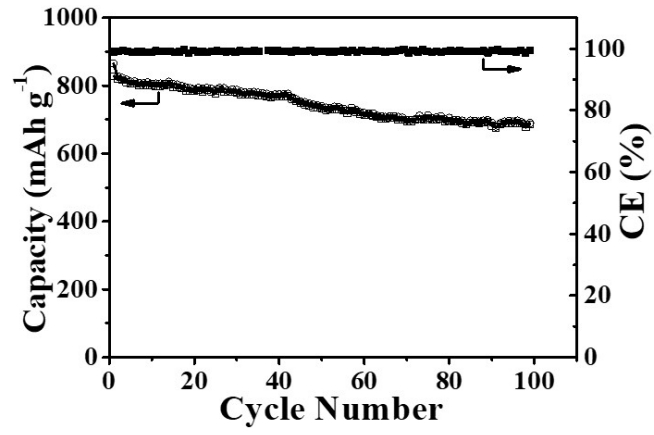


Fig. S11 Cycling performance of P-SnO₂/C@NC at the current density of 0.4 A g⁻¹.

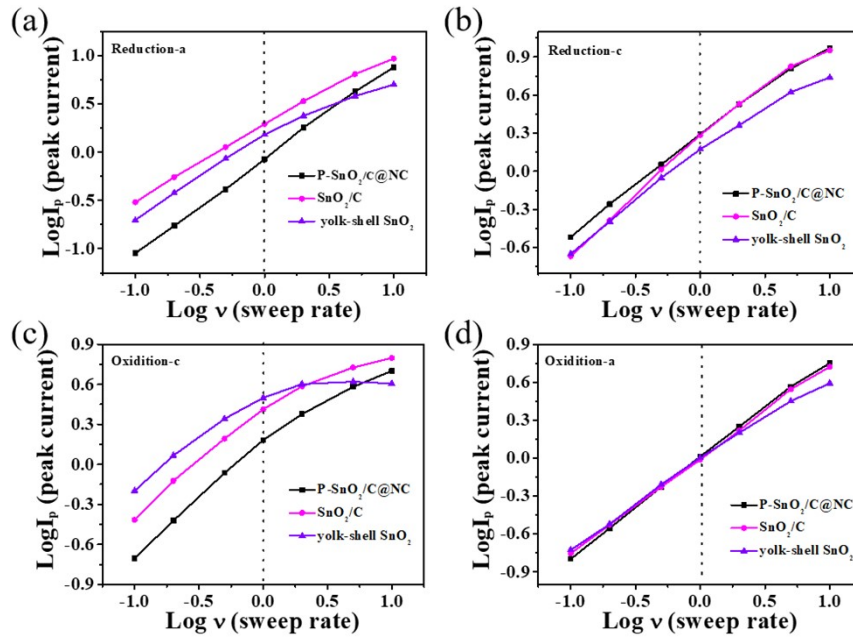


Fig. S12 Plots of $\log i$ versus $\log v$ curves of cathodic and anodic peaks in P-SnO₂/C@NC, SnO₂/C and yolk-shell SnO₂ electrodes. (a-d) correspond to the peaks of SnO₂→Sn, Sn→Li_xSn, Li_xSn→Sn and Sn→SnO₂ in Fig. 4, respectively.

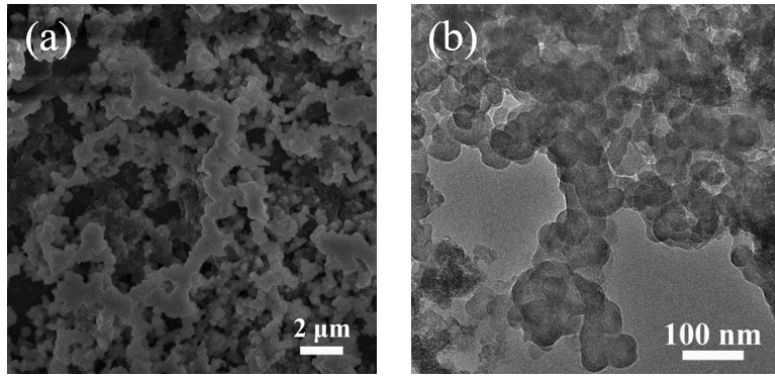


Fig. S13 (a) SEM and (b) TEM images of the yolk-shell SnO₂ electrode after 100 cycles.

Samples	0.1-1 mV s ⁻¹				1-10 mV s ⁻¹			
	re-a	re-c	oxi-c	oxi-a	re-a	re-c	oxi-c	oxi-a
P-SnO ₂ /C@NC	0.97	0.81	0.89	0.81	0.95	0.68	0.52	0.75
SnO ₂ /C	0.96	0.82	0.82	0.74	0.68	0.65	0.38	0.75
yolk-shell SnO ₂	0.83	0.91	0.70	0.74	0.58	0.41	0.10	0.59

Table S1 The calculated b values obtained from the slope of the plot of log i vs log v for P-SnO₂/C@NC, SnO₂/C and yolk-shell SnO₂ electrodes at the scan rates of 0.1-1 mV s⁻¹ and 1-10 mV s⁻¹.